Evaluating Silica Scaling in Enhanced Geothermal Systems Under Dispatchable Scenarios for Both Conventional and Waste Heat Injection Scenarios

Georgia Caruso Carter, Rita Esuru Okoroafor and Roman J. Shor

Harold Vance Department of Petroleum Engineering, Texas A&M University, College Station, TX, USA

georgiacarusocarter@tamu.edu

Keywords: dispatchable energy, enhanced geothermal systems, silica scaling, waste heat

ABSTRACT

With the development of technology for enhanced geothermal energy, there is a growing potential for its application in dispatchable geothermal energy. Dispatchable energy has the added benefit of optimized economics, with the ramping up of production during high energy demand and high energy prices and reduction of production during low demand and energy prices. As enhanced geothermal systems tend to target granite layers for their reservoir, silica scaling is a growing concern. The injection of cold water in the fractured system causes the silica to precipitate out of solution in the reservoir, decreasing flow and accelerating the thermal drawdown as silica scaling acts as an insulator. This paper evaluates the subsurface effects of the cyclical pressure and temperature changes, that are a result of the nature of dispatchable geothermal energy, and its effect on silica scaling in the reservoir. A non-isothermal reservoir numerical simulator was applied to develop a reservoir model of an enhanced geothermal system in an artificially stimulated granite reservoir. The model evaluates thermal-hydraulic flow, time-dependent heat transport, and geochemical equilibrium calculations for silica solubility. A variety of multiple production-rest cycles are evaluated, as well as waste heat storage to evaluate optimal production scenarios. The simulation results stress the importance of accounting for silica scaling in enhanced geothermal systems, particularly in dispatchable production cases. Optimal operational thresholds are defined for the typical multiple production-rest case, as well as for the waste heat storage case. These thresholds decrease the need for scaling intervention and decrease the production losses associated with the scaling.

1. INTRODUCTION

1.1 Industrial Waste Heat Potential

Industrial waste heat is defined as heat rejected from energy intense processes to produce high value-added products (Papapetrou et al., 2018). Within the EU and UK alone, in 2021 there was an estimated waste heat potential of 221.32 TWh/y, with more than half of the waste heat in the range of 100°C-200°C (Kosmadakis, 2024). There are various opportunities to use the waste heat, whether it is for direct heat recovery, waste heat to power, heat upgrading (Kosmadakis, 2024, Miró et al., 2016, Kosmadakis et al., 2020, Xu et al., 2019). However, with each solutions different issues arise, two prominent ones are the discrepancy between heat demand and supply locations, as well as investment cost and space for the heat recovery facility (Xu et al., 2019, Miró et al., 2016). This paper aims to assess the technical feasibility of repurposing the waste heat in the form of direct heat recovery to be used to slow down the thermal drawdown of the dispatchable EGS reservoir. By using an enhanced geothermal system (EGS) combined with dispatchability, this paper addresses the barriers of industrial heat waste usage. EGS are more flexible than classical geothermal systems, in that they do not require water in place nor favorable permeabilities as the permeability is introduced into the hot dry rock through hydraulic fracturing (Cladouhos et al., 2016). To decrease the costs, dispatchability is used as the production method for the reservoir. By injecting during low energy prices and demand, and producing during high energy prices and demand, the economics of a geothermal system are optimized. Aljubran and Horne's 2025 paper found up to a 10% increase on return on investment (ROI) in flexible dispatch production (Aljubran and Horne, 2025).

1.2 Silica Scaling in EGS

EGS projects commonly target granite rich reservoirs as was the case for the Haute-Sorne EGS pilot in Switzerland (Meier and Zingg, 2025) and the EGS Soultz Site in France (Hooijkaas et al., 2006). Silica reacts with the water with the following equation

$$SiO_{2\,(s)} + 2H_2O_{(l)} \leftrightarrow H_4SiO_{4\,(aq)} \tag{1}$$

(Rimstidt and Barnes, 1980). Within the context of this paper, amorphous silica is modelled instead of its crystalline counterpart, quartz, as it is more reactive for temperatures below 260°C (Pandey et al., 2015). Whilst there is plenty of research on dispatchable EGS(Ricks et al., 2022, Ricks et al., 2025, Aljubran and Horne, 2025) and on silica scaling in geothermal systems (Pandey et al., 2015, Ontoy et al., 2003, Rutqvist et al., 2020), silica scaling in dispatchable EGS remains relatively under researched. The authors' previous paper stresses not only that silica scaling must be included in reservoir simulations of EGS in granite, but also that there are drastic differences between baseload silica scaling (Caruso Carter et al., 2026).

1.3 Effect of Injecting Waste Heat into the Reservoir

For waste heat storage, much hotter temperatures than usual is injected back into the reservoir. By doing so, this delays the thermal drawdown of the reservoir, extending the reservoir's life, however, it is important to assess the effect on the chemical reactions. The higher the temperature, the more silica can be dissolved in the water, this relationship can be seen in the following equation

$$log \ K = -0.369 - 7.890 \times 10^{-4} \times T - \frac{3438}{T} \tag{2}$$

where the equilibrium constant K is a function of temperature in Kelvin (Rimstidt and Barnes, 1980). Nonetheless, temperature also influences the reaction rate. The reaction rate, k_-, of all silica phases' precipitation in water and its temperature dependence was obtained experimentally from the same paper as

$$log \ k_- = -0.707 - \frac{2598}{T} \tag{3}$$

(Rimstidt and Barnes, 1980). Pandey et al.'s paper investigated the effect of temperature and silica concentration in the injected water on silica precipitation in an EGS. Their results support Rimstidt and Barnes' 1980 paper that temperature had a larger effect on the silica falling out of solution instead of the degree of supersaturation (Pandey et al., 2015). However, there is a lack of research on how dispatchability affects the silica precipitation with varying injection temperatures under dispatchable production. This paper aims to provide more insight the effect of dispatchability, to help further understand how geothermal energy can play a role in waste heat storage.

2. METHODOLOGY

ECLIPSE was used to evaluate the thermal-hydraulic flow, time-dependent heat transport, and geochemical equilibrium calculations for silica solubility in the geothermal reservoir. ECLIPSE is an established reservoir simulation software, that has been validated for its uses in geothermal reservoir modelling (Stacey and Williams, 2017).

2.1 Building the Model

This work replicates Caruso Carter et al.'s 2026 reservoir model. The model is made up of 50 x 50 x 45 grid blocks, representing a volume of 1000 m x 1000 m x 191.105 m situated 1704.45 m deep in the subsurface. There is a single horizontal fracture at a depth of 1800 m spanning across the X and Y direction at grid block depth 23. The X and Y direction have consistent grid block lengths of 20 m, whilst in the Z direction the grid block length is 5 m with a symmetrical refinement from both directions approaching the fracture. The system being modelled is a tight granite reservoir, which is why a low permeability of 10^{-18} was selected, restricting the flow to the fracture. Further information regarding the reservoir parameters can be found below in Table 1. The injector is in the middle of the grid at coordinates (25,25,23) and the producer is at (45,25,23), both perpendicular to the fraction. A trace amount of silica is dissolved in the injected water. Figure 1 is provided below to provide clarity regarding the model's set up.

Table 1: Reservoir modelling parameters.

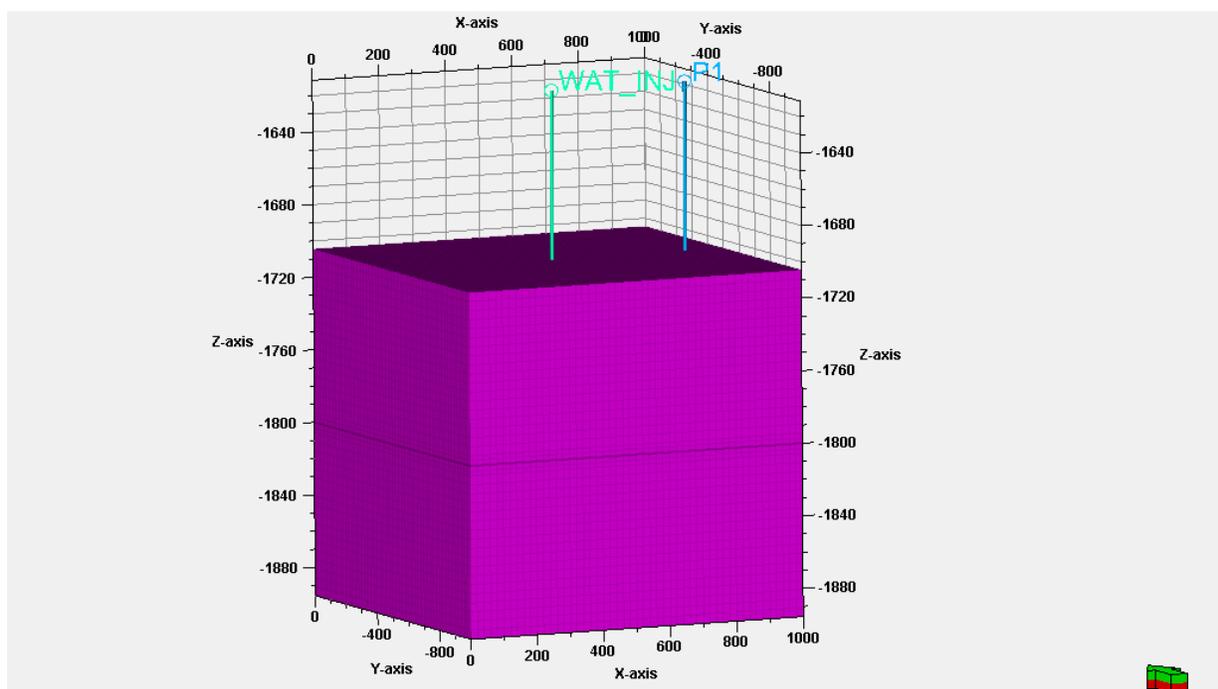| Property	Value	Unit
Initial fracture aperture	5	mm
Rock permeability	10^{-18}	m^2
Rock matrix porosity	0.01	-
Rock density	2500	kg/m^3
Fluid heat capacity	4180	J/kg/K
Rock thermal conductivity	2.5	W/m/K
Fluid thermal conductivity	0.6	W/m/K
Reservoir temperature at fracture	260	°C
Mass flow rate	40	kg/s
Injected water silica concentration	0.0056	mol/kg

Figure 1: The reservoir as constructed in ECLIPSE, with the injector (WAT_INJ) at coordinates (25,25,23) and producer (P1) at (45,25,23).

2.2 Injection Parameters

This paper investigates the dispatchable production of energy for enhanced geothermal systems. To stimulate varying demand for electricity, a production cycle of 12 hours with 40 kg/s injection and 20 kg/s production, followed by 12 hours with 20 kg/s injection and 40 kg/s production. By producing at higher rates during times of high demand, and thus high electricity prices and vice versa for injection, the system can be optimized to maximize profit. The production/injection was not stopped completely, instead it is at a 50 % reduction to prevent drastic saturation changes within the model. To fully evaluate the effect of the silica scaling, the silica is injected at an undersaturated concentration of 0.0056 mol/kg for the temperatures of water being injected. This value is far below the equilibrium concentration of 0.022 mol/kg at the fracture temperature using Equation 2. This concentration was selected as it is undersaturated for both the injection cases; however, further investigation with varying saturations would be interesting to evaluate in future research. As per Equation 3, the rate of precipitation is 6.66 times faster at 150°C compared to 100°C. This will provide sufficient contrast to understand how increasing the temperature of injected fluid will affect the geochemical reactions in the fracture.

3. RESULTS

3.1 Comparing the Results to Rimstidt and Barnes' 1980 Equation

To compare the effect of increasing the temperature, the results were evaluated with Equation 3. In Figure 2, the solid saturation at the injector grid block (25,25,23) were plotted. To validate the results against Equation 2, 150°C predicted was also plotted. As discussed in section 2.2, the 150°C should be 6.66 times faster than that at 100°C. The predicted value follows the trend of the 150°C case rather well, with a slight deviation. The deviation is due to the prediction assuming a constant 150°C temperature at the grid block, thus not accounting for the heat transfer from the 260°C reservoir. Nonetheless, Figure 2 shows as predicted that in a pure water and silica environment with the temperature ranges of 100°C and 260°C, the temperature has a greater effect on the rate of the precipitation reaction rather than the degree of undersaturation.

3.2 Saturation for the 100°C and the 150°C Cases

Figure 3. shows the solid saturation distribution after 1-5 years for both the 100°C and the 150°C case. In both cases there is a ring of solid precipitation surrounding the injector, with the greatest concentration of the solid to the right of the producer. It is evident that there are discrepancies in how the solid saturation is distributed between the two cases. For the 150°C, the thickness of the solid saturation band around the injector is far thicker and has a higher concentration of solid silica precipitation compared to the 100°C case. This is due to two factors, a faster rate of reaction due to the increased injection temperature, as well as in increased mobility of the fluid. As predicted from Equation 2, the solid silica precipitation is higher due to the higher temperature, making the rate of reaction faster than that of the 100°C case. Assuming the permeabilities of the two cases remain constant, the mobility ratio for the 150°C case is higher due to the temperature dependence of viscosity. This allows for the cold water front to invade a larger area of the reservoir, thus causing the silica to come out of solution as the reservoir fluid is fully saturated with silica at initial reservoir conditions..
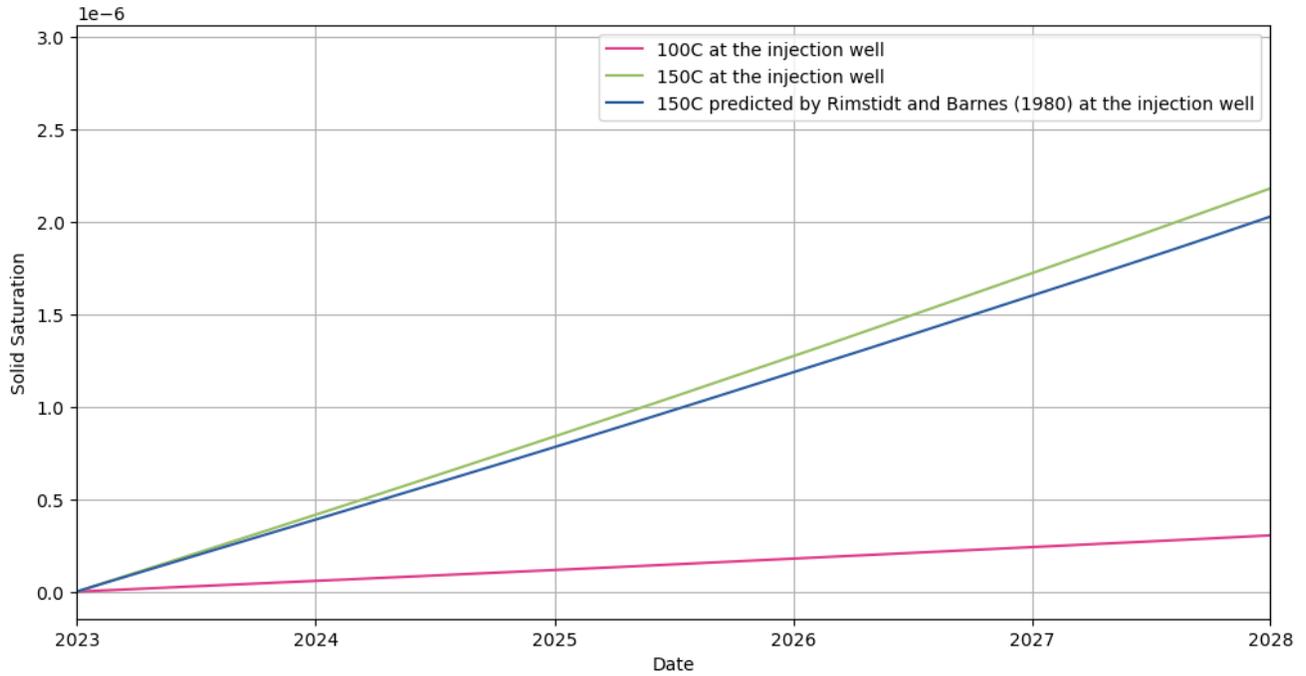
Figure 2: Solid saturation at the injection well for the 100°C, 150°C, and the predicted 150°C case. The predicted case uses Rimstidt and Barnes' 1980 equation, where the reaction rate at 150°C is 6.6 times faster than that at 100°C.
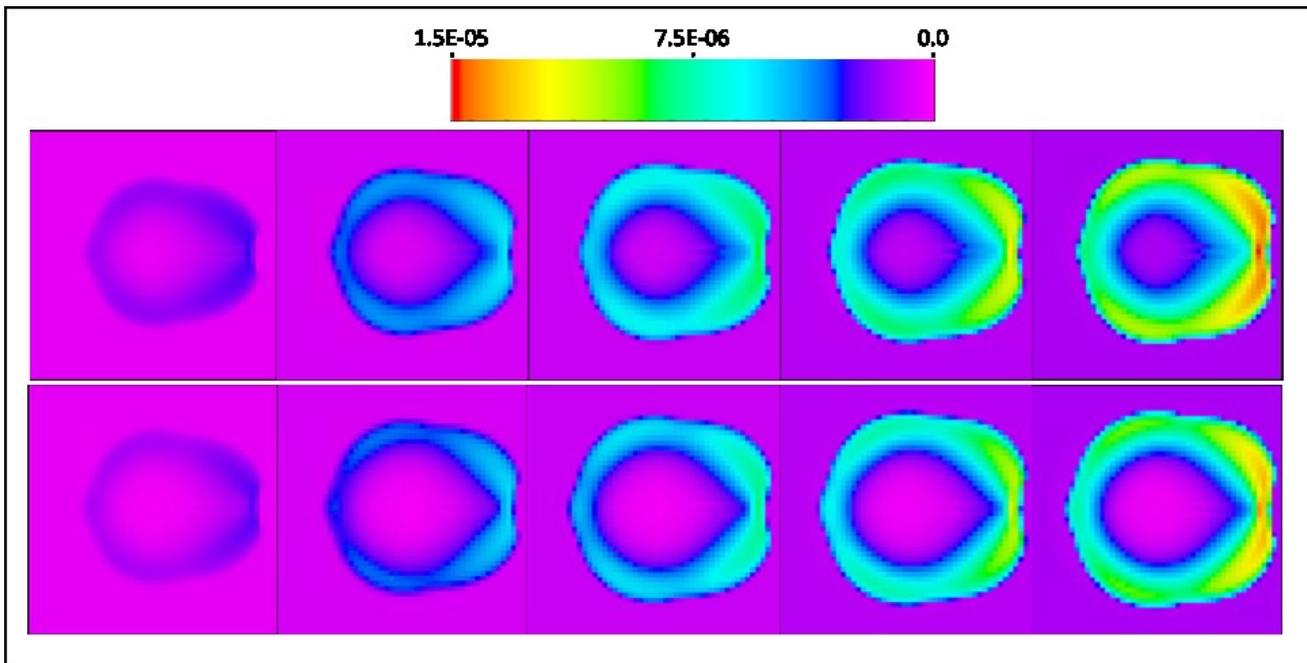

Figure 3. Top - 150°C case: from left to right the solid silica saturation is seen after 1 year, 2 years, 3 years, 4 years and 5 years. Bottom - 100°C case: from left to right the solid silica saturation is seen after 1 year, 2 years, 3 years, 4 years and 5 years.

3.3 Temperature for the 100°C and the 150°C Cases

In Figure 4. the differences between the temperature profiles at the fracture can be seen. As expected, the 100°C case has created a larger cooled region at a faster rate than that of the 150°C. Despite the increased mobility of the 150°C case, the 100°C has caused a greater decrease due to the larger difference in temperature between the injected fluid and the reservoir temperature.
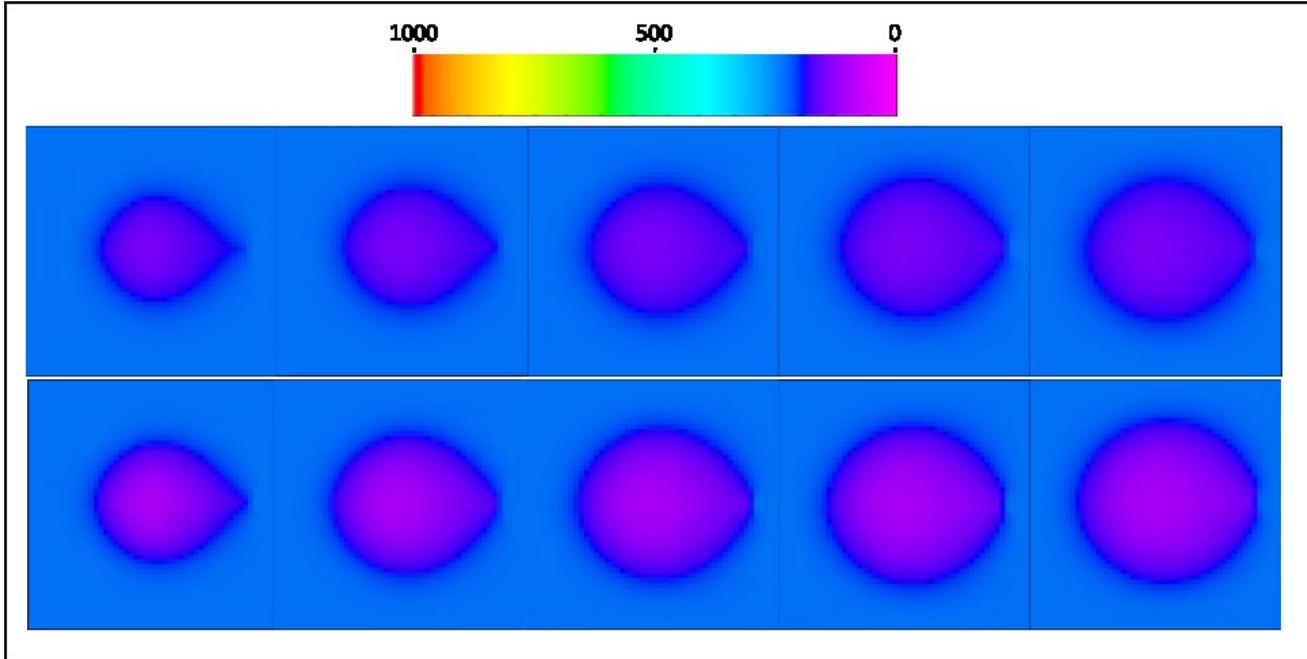

Figure 4. Top - 150°C case: from left to right the temperature at the fracture is seen after 1 year, 2 years, 3 years, 4 years and 5 years. Bottom - 100°C case: from left to right the temperature at the fracture is seen after 1 year, 2 years, 3 years, 4 years and 5 years.

4. DISCUSSION

This paper provides an initial understanding of the complex interactions of silica precipitation under dispatchable EGS for waste heat storage. The effect of waste heat injection was tested at two different temperatures, 150°C and 100°C, to evaluate the effect on the silica precipitation for the initial five-year period of the EGS's life. The simulations were run on Eclipse, with a doublet system connected by a single horizontal fracture in a granite reservoir. The dispatchable cycle was a 12-hour production at 40 kg/s and injection at 20 kg/s, followed by a 12-hour production at 20 kg/s and 40kg/s injection of undersaturated water into a fully silica saturated reservoir. The results showed that injecting at 150°C was less favorable than injecting at 100°C, this is due to the increased precipitation rate, as well as the increased mobility of the fluid. The increased mobility meant that regions in the reservoir were contacted by the colder water front sooner with the 150°C case than that of the 100°C case. Overall, geothermal energy is a viable option for direct heat use of the waste industrial heat, with this paper showing that higher injection temperatures may not be more beneficial for the EGS. This paper provides an initial analysis of optimizing waste heat usage for geothermal energy, opening the door for further optimization in terms of greater temperature intervals, longer time periods as well as different production regimes.

REFERENCES

ALJUBRAN, M. J. & HORNE, R. N. 2025. Techno-economics of geothermal power in the contiguous United States under baseload and flexible operations. *Renewable and Sustainable Energy Reviews,* 211**,** 115322.

CARUSO CARTER, G., OKOROAFOR, R. E. & SHOR, R. J. 2026. Silica Scaling in Dispatchable Enhanced Geothermal System Modelling. *World Geothermal Congress 2026* Calgary, Canada.Accepted

CLADOUHOS, T. T., PETTY, S., SWYER, M. W., UDDENBERG, M. E., GRASSO, K. & NORDIN, Y. 2016. Results from Newberry Volcano EGS Demonstration, 2010–2014. *Geothermics,* 63**,** 44-61.

HOOIJKAAS, G. R., GENTER, A. & DEZAYES, C. 2006. Deep-seated geology of the granite intrusions at the Soultz EGS site based on data from 5km-deep boreholes. *Geothermics,* 35**,** 484-506.

KOSMADAKIS, G. 2024. Industrial waste heat potential and heat exploitation solutions. *Applied Thermal Engineering,* 246**,** 122957.

KOSMADAKIS, G., ARPAGAUS, C., NEOFYTOU, P. & BERTSCH, S. 2020. Techno-economic analysis of high-temperature heat pumps with low-global warming potential refrigerants for upgrading waste heat up to 150 °C. *Energy Conversion and Management,* 226**,** 113488.

MEIER, P. & ZINGG, O. 2025. Status of Multi-Stage EGS and the Haute-Sorne Project in Canton Jura, Switzerland. 2025**,** 1-5.

MIRó, L., GASIA, J. & CABEZA, L. F. 2016. Thermal energy storage (TES) for industrial waste heat (IWH) recovery: A review. *Applied Energy,* 179**,** 284-301.

ONTOY, Y., MOLLING, P., XU, T., SPYCHER, N., PARINI, M. & PRUESS, K. 2003. Scaling of hot brine injection wells: supplementing field studies with reactive transport modeling. *Lawrence Berkeley National Laboratory***,** 2003-1.

PANDEY, S. N., CHAUDHURI, A., RAJARAM, H. & KELKAR, S. 2015. Fracture transmissivity evolution due to silica dissolution/precipitation during geothermal heat extraction. *Geothermics,* 57**,** 111-126.

PAPAPETROU, M., KOSMADAKIS, G., CIPOLLINA, A., LA COMMARE, U. & MICALE, G. 2018. Industrial waste heat: Estimation of the technically available resource in the EU per industrial sector, temperature level and country. *Applied Thermal Engineering,* 138**,** 207-216.

RICKS, W., NORBECK, J. & JENKINS, J. 2022. The value of in-reservoir energy storage for flexible dispatch of geothermal power. *Applied Energy,* 313**,** 118807.

RICKS, W., VOLLER, K., GALBAN, G., NORBECK, J. H. & JENKINS, J. D. 2025. The role of flexible geothermal power in decarbonized electricity systems. *Nature Energy,* 10**,** 28-40.

RIMSTIDT, J. D. & BARNES, H. L. 1980. The kinetics of silica-water reactions. *Geochimica et Cosmochimica Acta,* 44**,** 1683-1699.

RUTQVIST, J., PAN, L., SPYCHER, N., DOBSON, P., ZHOU, Q. & MENGSU, H. Coupled Processes Analysis of Flexible Geothermal Production from Steam-and Liquid-Dominated Systems: Impact on Wells. 45th Workshop on Geothermal Reservoir Engineering, 2020 Stanford, California.

STACEY, R. W. & WILLIAMS, M. J. 2017. Validation of ECLIPSE reservoir simulator for geothermal problems. *GRC Transactions.*

XU, Z. Y., WANG, R. Z. & YANG, C. 2019. Perspectives for low-temperature waste heat recovery. *Energy,* 176**,** 1037-1043.